Title

Nitric Oxide Releasing Materials Triggered by Near-Infrared Excitation Through Tissue Filters

Journal

Journal of the American Chemical Society, 135(48)

ISSN

0002-7863

Authors

Burks, Peter T

Garcia, John V

GonzalezIrias, Ricardo

et al.

Publication Date

2013-12-04

DOI

10.1021/ja408516w

Peer reviewed

JACS
JOURNAL OF THE AMERICAN CHEMICAL SOCIETY
Article
pubs.acs.org/JACS

Nitric Oxide Releasing Materials Triggered by Near-Infrared Excitation Through Tissue Filters

Peter T. Burks,[⊥,†] John V. Garcia,[⊥,†] Ricardo GonzalezIrias,[†] Jason T. Tillman,[†] Mutong Niu,[‡] Alexander A. Mikhailovsky,[†] Jinping Zhang,[‡] Fan Zhang,[§] and Peter C. Ford*[,†]

[†]Department of Chemistry and Biochemistry, University of California, Santa Barbara, Santa Barbara, California 93106-9510, United States

[‡]Suzhou Institute for Nanotech and Nanobionics, Suzhou Industrial Park, Suzhou, China

[§]Department of Chemistry and Laboratory of Advanced Materials, Fudan University, Shanghai 200433, PR China

Supporting Information

ABSTRACT: Novel materials for the phototherapeutic release of the bioregulator nitric oxide (nitrogen monoxide) are described. Also reported is a method for scanning these materials with a focused NIR beam to induce photouncaging while minimizing damage from local heating. The new materials consist of poly(dimethylsiloxane) composites with near-infrared-to-visible upconverting nanoparticles (UCNPs) that are cast into a biocompatible polymer disk (PD). These PDs are then impregnated with the photochemical nitric oxide precursor Roussin's black salt (RBS) to give UCNP_RBS_PD devices that generate NO when irradiated with 980 nm light. When the UCNP_RBS_PD composites were irradiated with NIR light through filters composed of porcine tissue, physiologically relevant NO concentrations were released, thus demonstrating the potential of such devices for minimally invasive phototherapeutic applications.

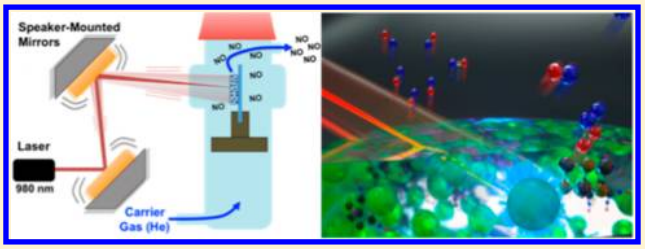

INTRODUCTION

Photochemical delivery of therapeutic substances offers control over location, timing, and dosage through modulation of the light source.[1] Furthermore, the applicability of this method is enhanced when tissue-transmitting wavelengths in the near-infrared (NIR) region can be utilized to trigger such delivery.[2,3] One important therapeutic molecule is nitric oxide (nitrogen monoxide), and we describe here new NO-releasing polymer disks (PD) that are activated with NIR light. This PD consists of a poly(dimethylsiloxane) (PDMS) matrix into which lanthanide-based upconverting nanoparticles (UCNPs) have been incorporated. UCNPs generate visible wavelength emission when multiple Yb^{3+} sensitizer ions absorb NIR light and undergo sequential energy transfer to populate higher energy, emissive excited states in acceptor/emitter ions such as Er^{3+} or Tm^{3+}.[4] Reabsorption of that emission triggers NO release from a precursor infused into the same biocompatible material. The photoNORM (photoactivated NO releasing moiety) used here is the iron cluster $[NH_4][Fe_4S_3(NO)_7]$, known as Roussin's black salt (RBS, see Figure S-1 of the Supporting Information).[5] This system should also be readily adaptable to incorporating other photoNORMs or photochemical precursors for various bioactive small molecules.[6]

Nitric oxide is an endogenous mammalian bioregulator with established roles in vasodilation, immune response, and tumor growth and suppression.[7] In addition, it sensitizes γ-radiation killing of hypoxic cells.[8] Thus, there is considerable interest in controlled therapeutic delivery of NO.[9] The use of implants containing a thermally activated NO precursor provides a method for localized therapeutic applications, and this has drawn the attention of other researchers.[10] Photochemically triggered release of a caged drug provides precise temporal and dosage control, while spatial control depends in part on the ability of the precursor to localize at the desired site. The PDs described here would allow one to define the location while using photoactivation by NIR light to define the timing and dosage.

Effective use of photochemical uncaging of bioactive molecules is limited by poor tissue transmission of UV and shorter visible wavelengths, the therapeutic window being ~650−1350 nm.[11] This feature has stimulated interest in our laboratory and others in nonlinear methodologies, such as two-photon excitation and NIR-to-visible upconversion, as ways to access the excited states necessary for uncaging bioactive agents such as NO,[12−14] as well as for deep tissue imaging.[15] Upconversion has the advantage that excitation is achieved with a simple continuous wave NIR diode laser, but preparing molecular or supramolecular species combining all the desired properties with photochemical lability is synthetically challenging. In the alternative described here, an implantable solid material encapsulates separate components in a biocompatible

Received: August 22, 2013
Published: November 18, 2013

   dx.doi.org/10.1021/ja408516w | J. Am. Chem. Soc. 2013, 135, 18145−18152

matrix, thus allowing UCNP and NO precursor to be concentrated together in a polymer disk (PD). This encapsulation also isolates the components from the external medium, thereby reducing toxicity. Such a device would be a stable, NIR active, photochemical NO delivery material that can be implanted in a desired location and triggered on demand using tissue-penetrating NIR light (Figure 1). The effectiveness of NIR irradiation was tested by using "filters" made from porcine tissue.

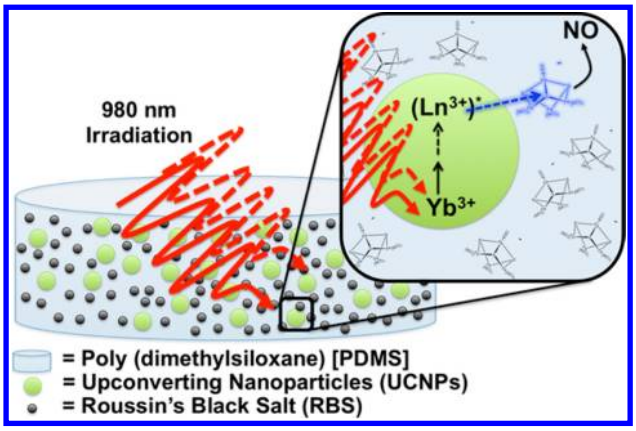

Figure 1. Cartoon depicting how the photochemically active NO releasing polymer disks (PDs) are proposed to function. NIR light excitation of the UCNPs results in visible emission that is absorbed by the photochemical precursor (RBS in this case) triggering the release of NO.

EXPERIMENTAL SECTION

Experimental details regarding the synthesis and characterization of the UCNPs and PDMS disks used in these studies are summarized in Tables S-1−S-3 and Figures S-2−S-12 of the Supporting Information. Methods for photochemical generation and analysis of the NO are described in the following sections.

RESULTS AND DISCUSSION

Fabrication of PD Devices. These have three key components: the polymer matrix, the UCNPs, and the RBS. The PDMS matrix is biocompatible[16] and FDA approved for in vivo use.[17] Furthermore, PDMS is moldable, is transparent to visible and NIR light (Figure S-11 of the Supporting Information), and is hydrophobic.[18] This last property allows for lipophilic substrates to be infused into the porous polymer by incubating preformed PDs in a compatible organic solvent containing the photoNORM. After solvent removal, the hydrophobicity traps the substrates in the polymer matrix with minimal leaching into aqueous solution. For example, RBS, the photoNORM used here, is soluble in diethyl ether, but once infused into the PDs, does not appreciably leach into aqueous media.

The upconverting nanoparticle cores were composed of $Na(Y/Gd)F_4$ doped with Yb^{3+} as the NIR light harvesting chromophore and sensitizer and with either Er^{3+} or Tm^{3+} as the light emitters. The visible emissions from these UCNPs nicely overlap the broad absorption bands of RBS (Figure 2).[13]

Three compositions of $Na(Y/Gd)F_4$ UCNPs (20% Gd, 20% Yb, and 2% Er), (20% Gd, 30% Yb, and 2% Er), and (20% Gd, 20% Yb, and 0.2% Tm), each coated with a thin shell of $NaYF_4$ to improve optical performance,[19] were used. These were prepared using a high throughput robotic system at the

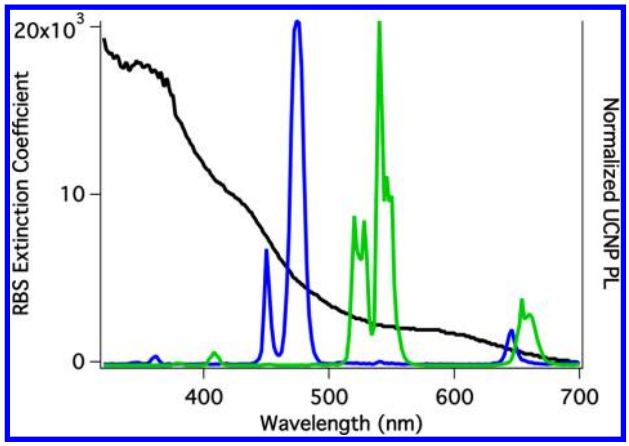

Figure 2. Overlay plot of RBS absorption extinction coefficient (black line) versus the UCNP photoluminescence (Tm-UCNP: blue line and Er-UCNP: green line) depicting the spectral overlap between the upconversion emission of the UCNPs and absorption of the RBS acceptor.

Molecular Foundry,[20] using procedures adapted from Ostrowski et al[21] with modest modifications.[22,23] Synthesis and characterization procedures are described in the Supporting Information. Each UCNP sample was of the hexagonal (β) crystal phase (Figures S-2 and S-3 of the Supporting Information), and TEM studies at the Suzhou Institute for Nanotech and Nanobionics showed each batch to be monodisperse (Figures S-4−S-7 and Table S-2 of the Supporting Information).

Upconversion quantum yields (QY) for emission in the 400−550 nm range, measured using the method of Boyer and van Veggel,[24] were quite small (at 60 W/cm^2) but increased with particle diameter and excitation power (Table S-3 of the Supporting Information). The higher Yb^{3+} concentration gave substantially larger UCNP diameters, thus, improving upconversion effectiveness both by increasing the NIR absorption and by directing larger particle growth.

The PDs were prepared by suspending a sample of UCNPs (0 to 10 mg, see the Supporting Information)[25] in the viscous liquid PDMS precursor (50 μL Dow Sylgard 184) in the disk molds (Figure S-9 of the Supporting Information). These mixtures were cured at 383 K for 1 h, then at ambient temperature for 10 h (see the Supporting Information). The resulting PDs are 5 mm in diameter and 2 mm thick but displayed some inhomogeneity in UCNP distribution. The photoNORM was then infused into these PDs by soaking in an ether solution of RBS (NH_4^+ salt, 40 mg/mL) in an oxygen-free glovebox for 5 min. The solvent was then removed under low pressure. The procedure was repeated 3 more times for each PD with resulting color change (clear to black), indicating that RBS had infused into the PDs (Figure S-10 of the Supporting Information). After multiple washes with water and phosphate-buffered saline solution, the infused RBS did not leach appreciably into aqueous media. On the basis of UV−visible absorption spectroscopy, the infused PDs contained approximately 50 nmols of RBS corresponding to ~350 nmols of NO available per PD device. Once fabricated and dried under low pressure, the UCNP_RBS_PDs were stored under inert atmosphere until used, and under these conditions, the PDs were stable for months.

dx.doi.org/10.1021/ja408516w | J. Am. Chem. Soc. 2013, 135, 18145−18152

The PD devices thus prepared are listed in Table 1. The labeling designates the types of UCNP cores and identifies the emitting ions present.

Table 1. Designations and UCNP Core Compositions of PD Devices, Each Infused with RBS As Described

device	UCNP core composition[a] and diameter	
A(Er)[b]	(20% Gd, 20% Yb, and 2% Er)	7.3 nm
B(Er)[b]	(20% Gd, 30% Yb, and 2% Er)	12
C(Tm)[b]	(20% Gd, 20% Yb, and 0.2% Tm)	10.8
D(Tm)[c]	(20% Gd, 20% Yb, and 0.2% Tm)	10.8
E(0)	no UCNPs used	–

[a]$NaYF_4$ UCNPs with these percentages of other cations in the cores, each with a $NaYF_4$ shell. [b]Five milligrams of the UCNP. [c]Ten milligrams of the UCNP.

Testing of PD Devices. *Durability under Photolysis.* The durability of the PDMS polymer matrix to the NIR excitation wavelengths was tested by subjecting a PD (prepared as above but without added RBS or UCNPs) to irradiation by a focused beam (0.8 mm diameter) of 980 nm light with the intensity of the beam at ~1000 W/cm^2.[26] The cured polymer displayed no visible damage from a 5 min exposure to this high-powered irradiation. The transparency of PDMS at this wavelength was shown by the absence of absorbance between 400 and 1100 nm using a Perkin-Elmer LAMBDA 750 UV−vis/NIR spectrophotometer.

Photoactivity of RBS in a PD. PDMS PDs without UCNPs were loaded with RBS as described above. These E(0) PDs (Table 1) were mounted in a photolysis flow cell designed to hold the polymer disk in a reproducible, rigid configuration with an optical glass window through which the excitation beam is directed (Figure S-12 of the Supporting Information) to the mounted PD. The cell is designed so that a carrier gas transports any NO released to a Sievers Nitric Oxide Analyzer (NOA). Irradiation of these E(0) PDs with a 540 nm LED (~7 mW) released NO in quantities linearly proportional to the photolysis time intervals (5 to 40 s, Figure S-13 of the Supporting Information). This is consistent with the known solution photochemistry of RBS.[7b] Thus, RBS, once infused into the PDs, remains photochemically active, and the NO generated is readily released from the polymer matrix.

NIR Excitation of PDs. The ability of a thulium-based UCNP_RBS_PD to release NO under NIR excitation was demonstrated with the D(Tm) PD in the same photolysis flow cell but using a 980 nm diode laser with the beam expanded to a 5 mm diameter as the excitation source. Figure 3 illustrates the NO released as a function of the length of the photolysis time-interval indicated. This result is consistent with the earlier observation by Garcia et al.[13] that 980 nm excitation of solutions containing both free RBS and erbium-based UCNPs generated significant quantities of NO. Free RBS alone in solution is insensitive to this excitation wavelength. Thus, the NO release can be attributed to NIR excitation of the UCNPs leading to visible range emissions that are reabsorbed by RBS.

An earlier study of RBS and UCNPs in solution[13] also showed that quantitative NO release has a nonlinear response to the intensity of the excitation source as does the upconverted visible emission. Thus, a much higher NO release could be expected for a higher intensity NIR beam, and this was accomplished by focusing to a diameter of ~0.8 mm to give an intensity ~40-fold greater than the expanded beam at the same

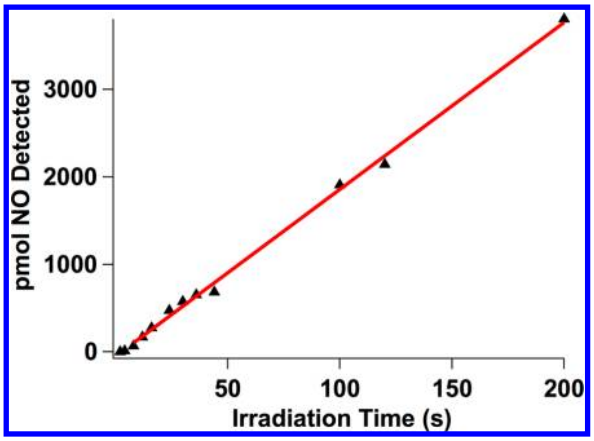

Figure 3. Plot of NO generated from the UCNP_RBS_PD D(Tm) photolyzed by a stationary 980 nm diode laser beam expanded to a 5 mm diameter (~2.5 W/cm^2). Each point represents the integrated NOA signal for NO generated during the photolysis for the time interval indicated.

total power. Doing this resulted in very substantial enhancement of the NO released. However, the inhomogeneous UCNP distribution in the PDs led to concern about quantitatively comparing samples, since the focused beam has a diameter much smaller than that of the PDs. Furthermore, when the tissue filter experiments (see below) were first attempted with the focused 980 nm laser beam, damage from localized heating was apparent within a few seconds.

Design of Oscillating Laser Beam Photolysis Apparatus. These concerns were the motivation for designing a novel optical train (Figure 4) that scans the focused excitation beam rapidly and repeatedly over the PD surface. This technique averages sample heterogeneity and minimizes localized heating effects. Movement is accomplished by reflecting the NIR beam off two mirrors, each mounted on a speaker oscillating under the control of a tunable function generator. This system simultaneously focuses and moves the excitation beam thereby

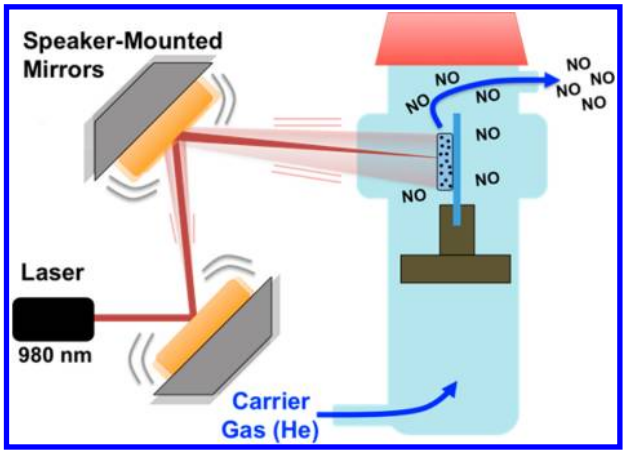

Figure 4. Cartoon depicting the optical train for photolysis of the PDs. Speakers driven by frequency generators oscillate the 980 nm diode laser beam in a scanning pattern over the UCNP_RBS PDs. The beam was moved in the '*X*' and '*Y*' directions using the two speaker-mounted mirrors, while simultaneously being focused onto the film to produce a high power density. Also depicted is the flow cell in which the sample is mounted where He carries any NO released to the NOA for detection. The mirrors were oscillated at 124 and 71 Hz, except where noted otherwise.

dx.doi.org/10.1021/ja408516w | J. Am. Chem. Soc. 2013, 135, 18145−18152

scanning the focal point over the surface of a PD sample mounted in the photolysis flow cell (Figures 4 and S-12 of the Supporting Information). The pattern of the oscillating beam was customized by tuning the frequency sent to each speaker. An example is Figure 5. Other examples are illustrated in Figure S-14 of the Supporting Information and in the video of the Supporting Information.

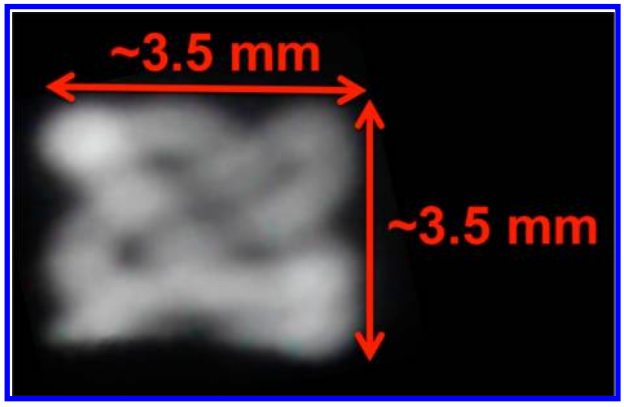

Figure 5. Patterns shown by an oscillating laser beam focused on a UCNP PD device mounted in the photolysis apparatus. The pattern is tailored by adjusting the frequency of each speaker using the function generator. The image shown is the emission from the UCNPs, recorded by a digital camera (shutter speed unknown). When integrated for a longer period, the image is filled.

Photolysis Studies of the PD Devices. All NIR photolysis experiments used a 980 nm diode laser for excitation and short wavelength cutoff filter to prevent spurious excitation from visible range second harmonics (490 nm). These experiments were performed in triplicate, so the reported values for NO release are the average of three runs.

Notably, a control experiment involving the 980 nm photolysis of PD E(0) (which does not contain UCNPs but is infused with RBS) with an oscillating laser beam (beam intensity at 400 W/cm^2) resulted in small, but detectable, NO release for irradiation intervals of 10 to 80 s (Figure S-15 of the Supporting Information). This was surprising since solutions of RBS show no photochemistry under similar NIR excitation.[13] The NO detected from these E(0) PDs was quite small [~7 pmoles (av) after 20 s irradiation] but was linearly proportional to the length of the photolysis interval. In addition, there was a noticeable decrease with each subsequent irradiation sequence. The mechanism responsible for this small NIR activity of RBS is unclear, but we suspect local heating effects due to impurities at the surface, especially since the residual NO release progressively decreases upon repeated experiments. Whatever the origin of this limited photosensitivity, the observed NO release was much less than seen in the presence of the UCNPs (see below).

PD devices A(Er), B(Er), C(Tm), and D(Tm) containing both UCNPs and RBS (Table 1) were similarly evaluated for NO release using this system. Dramatic enhancements of NO production were apparent for all four relative to E(0). For example, B(Er) generated ~1300 pmoles of NO during a 20 s photolysis interval of 980 nm irradiation (400 W/cm^2), several orders of magnitude larger than that seen under analogous conditions for E(0) (Figure S-16 of the Supporting Information). Indeed, photolysis intervals under these conditions longer than 20 s for B(Er) saturated the PMT detector of the NOA, thereby necessitating the use of the shorter irradiation times.

Figure 6 displays the NOA signal for the photolysis of A(Er) under similar conditions. The integrated signals gave 26, 95, 497, and 972 pmol NO for the photolysis times 2, 3, 5, and 7 s, respectively. Thus, unlike 540 nm photolysis of the E(0) PDs where the amount of NO released was proportional to the length of the irradiation interval, NO release from both A(Er) and B(Er) under 980 nm irradiation with the oscillating laser system is markedly nonlinear with excitation time.

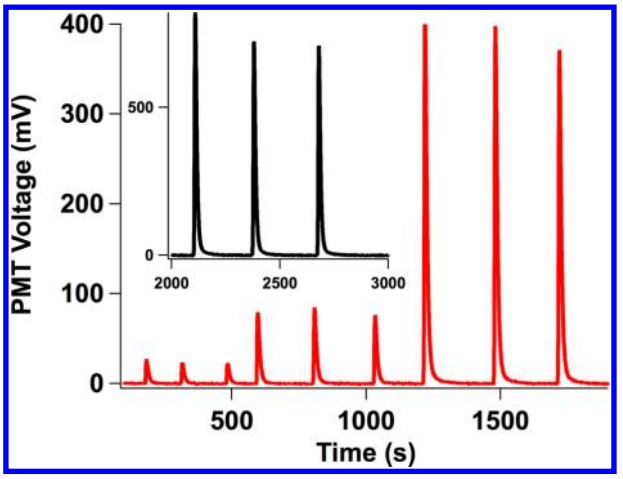

Figure 6. NOA data for 980 nm photolysis (200 W/cm^2) of device A(Er) for photolysis intervals of 2, 3, 5, and (inset) 7 s. The integrated NOA signals are proportional to the NO detected (in pmol).

This behavior also contrasts to that for solutions of UNCPs and RBS[13] with a stationary laser beam, from which NO production was linear with time, although nonlinear with laser power as expected for a process where the upconversion involves sequential multiphoton absorptions. We attribute the behavior of the current systems to a "charging" effect, whereas the more often the oscillating laser beam addresses a particular nanoparticle repeatedly within a short time frame (the beam is moving at an average speed of ~1 m s^{-1}), the higher the probability that it will stimulate the upconversion, which requires the excitation of multiple Yb^{3+} ion sensitizations. However, we have not yet developed an algorithm that predicts this behavior quantitatively for the current system.[27]

The UCNP_RBS_PDs C(Tm) (Figure 7) and D(Tm), using thulium as the visible emitter, were also highly sensitive to excitation at 980 nm. These were studied at 300 and 100 W/cm^2, respectively, the beam intensities being chosen to give optimum NO production for NOA analysis. For C(Tm), photolysis intervals between 1 and 7 s produced 3 to 995 pmol NO. For D(Tm), intervals from 10 and 80 s generated from 18 and 4200 pmol NO. Notably, these results were markedly nonlinear in terms of the production of NO as a function of the irradiation time using the oscillating diode laser beam. The data for the four sets of UCNP_RBS PDs are summarized in Table S-4 of the Supporting Information.

The nonlinear nature of the upconversion process makes direct quantitative comparisons of various systems difficult. As we and others have shown previously, the power dependence of the emission intensity from UCNPs similar to those shown here falls somewhere between 1.5 and second order, and this is also evident for reactions photosensitized by UNCPs.[11] In addition, the use of the oscillating laser excitation beam

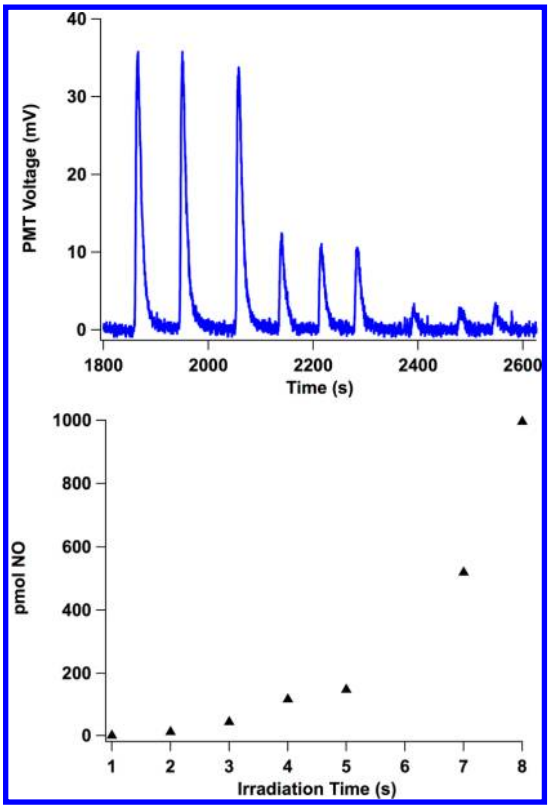

Figure 7. Top: NOA signal upon 980 nm photolysis of a C(Tm) UCNP_RBS PD with an oscillating diode laser beam at a focused intensity of 300 W/cm^2. The signals are for 3, 2, and 1 s photolysis intervals. Bottom: Plot of NO detected (in pmol) vs the photolysis time intervals for the same system.

incorporates some very interesting dynamics into the system, given the remarkable sensitivity of the NO production to the length of the photolysis interval (see below). However, a qualitative view of the relative behaviors of the four UCNP_RBS_PDs can be gained by examining the NO production at the same focused laser beam intensity (100 W/cm^2) and for the same photolysis time interval (40 s). Under these conditions, the amount of NO generated from A(Er), B(Er), C(Tm), and D(Tm) was 211, 52, 803, and 388 picomoles, respectively (see Table S-5 of the Supporting Information).[25] For comparison, only 6 picomoles of NO were generated by analogous excitation of the UCNP-free E(0) PD.

As noted above, nearly all of the samples studied here used the oscillating focused beam with the two mirrors operated at 121 and 71 Hz, respectively, since these conditions gave convenient concentrations with the NOA analysis method for these proof-of-principle studies. However, the nonlinear dependence of the NO release on the length of the photolysis interval suggests that further tuning of the technique may be necessary for defining the optimal NO release for a specific task. In order to determine qualitatively the effect of changing the beam oscillation frequency, three different oscillation frequencies were examined: 69 and 154 Hz, 34.5 and 77 Hz, and 17.25 and 38.5 Hz, with PD A(Er).

For a 10 s irradiation, this sample gave 18, 69, or 232 pmoles of NO, while a 20 s irradiation gave 60, 303, and 880 pmol of NO release for these respective frequency patterns. Clearly, slowing the oscillation frequency increases the NO release, while for all three examples, the NO release proved to be nonlinear with the irradiation time of the sample.

Luminescence Rise-Time and Decay Lifetime Measurements. These properties were measured for UCNP cores and core/shells as powders and for UCNP core/shells in the assembled PD devices using the NIR laser operating at 980 nm in the pulsed mode (see the Supporting Information for experimental details). Figure S-8 of the Supporting Information illustrates both processes for the emission at 473 nm of device C, which contains $NaYF_4$_(20% GD, 20% Yb, and 0.2% TM) core/shell UCNPs in the PDMS disk infused with RBS. Both the rise and decay of emission could be approximated as being exponential in character, and from the fits, the τ_r and τ_d values listed in Table 2 were calculated. These were measured for

Table 2. Rise-Time and Decay-Time Data for Several UCNP Cores, The Core/Shell Analogs, and for Same Core/Shell Species in the PD Devices

sample	τ_r (ms)	τ_d (ms)
Tm-UCNPs (λ_{em} 473 nm)		
^{core}UCNP powder[a]	1.33	0.57
^{CS}UCNP powder[a,b]	1.88	0.94
PD: C[a]	1.55	0.41
Er-UCNPs (λ_{em} 540 nm)		
^{CS}UCNP powder[c]	0.83	0.19
PD: B[c]	0.34	0.13
^{core}UCNP powder[d]	0.19	0.097
^{CS}UCNP powder[d]	1.06	0.21
PD: A[d]	0.30	0.13

[a]20% Gd, 20% Yb, and 0.2% Tm; core diameter = 10.8 nm. [b]"CS" refers to core/shell with a $NaYF_4$ shell. [c]20% Gd, 30% Yb, 2.0% Er; core diameter = 12 nm. [d]20% Gd, 20% Yb, 2.0% Er; core diameter = 7.3 nm.

several UCNPs at the wavelength λ_{em} at the strongest visible emission 473 nm for the UCNPs with Tm^{3+} as the emitting ion and 540 for those with Er^{3+} (Figure 2). Comparing the UCNP cores and the analogous cores with the $NaYF_4$ shells shows the latter to have a longer lifetime, consistent with the greater emission quantum yields for the core/shell constructs. Notably, the lifetimes for the core/shell species drop when they are in the polymer disks containing RBS. The reason for this is currently being probed in greater detail; however, one possible explanation would be that deactivation via energy transfer to the RBS chromophore contributes to the faster deactivation of the UCNPs. Such a mechanism could lead to more efficient photosensitization of the RBS chemistry than a simple upconverted emission−reabsorption pathway.

NIR Photolysis through Porcine Tissue Filters. One inspiration for using UCNP sensitizers was to develop NIR-active photochemical NO delivery materials that could be activated with irradiation through tissue. Thus, a noninvasive light trigger could control the timing and dosage of the therapeutic release. The effective photostimulated NO production from the UCNP_RBS_PDs listed in Table 1, in combination with the reported transparency to NIR light,[11] stimulated the design of experiments to test the efficacy of NO release from these materials when irradiated through tissue. Therefore, the previously described photolysis system was modified to allow placement of a tissue sample as a filter in the optical train immediately before the PD (Figure 8 and Figure S-17 of the Supporting Information). This system could be operated in three modes: with a nonoscillating focused 980 nm beam having a diameter of ∼0.8 mm, with the oscillating

dx.doi.org/10.1021/ja408516w | J. Am. Chem. Soc. 2013, 135, 18145−18152

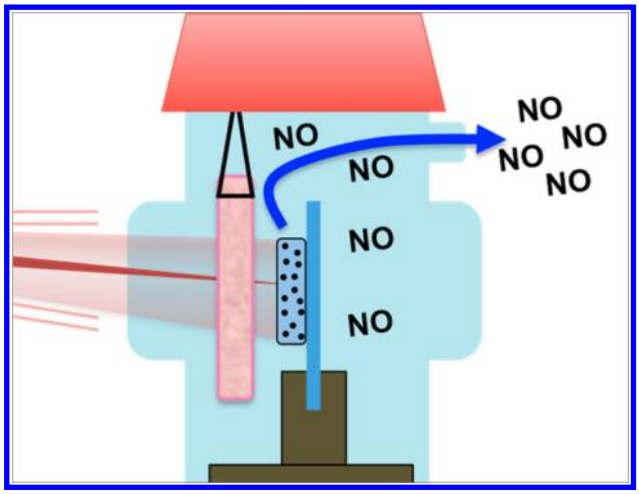

Figure 8. Zoomed-in perspective of the photolysis system described in Figure 3, depicting the modifications allowing for through-tissue photolysis. Localized heating is reduced by oscillating the beam as well as by placing the tissue filter (in pink) outside the focal point of the beam.

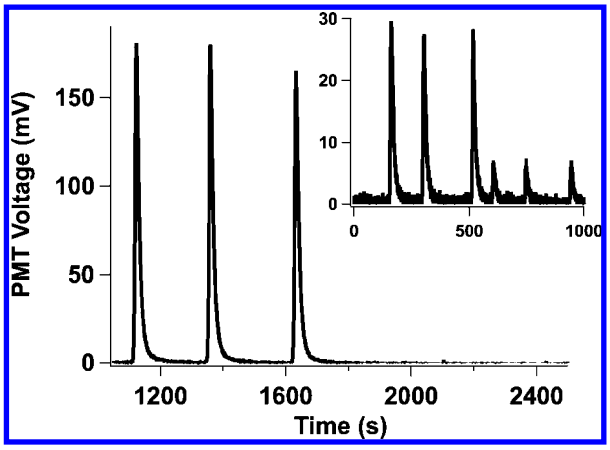

Figure 9. NOA data for 980 nm photolysis of a C(Tm) PD through a porcine muscle filter ~1.5 mm thick. Shown are 3 irradiation intervals of 10 s, resulting in an average of 300 pmol NO release. Inset: (left to right) 3 irradiation intervals each of 5 and 2.5 s length, resulting in average NO production of 48 and 11 pmol NO, respectively. In each case the intensity of the incident beam was 400 W/cm^2.

focused beam as described above, or with a defocused beam having a diameter of ~3 mm. The nonoscillating focused beam damaged ("cooked") the tissue samples (see Figure S-17 of the Supporting Information), so the studies reported here are concerned with the latter two approaches. Both operated at 2 W, with the respective power intensities at 400 (at the focal point) and 28 W cm^{-2}.

Three types of porcine tissue, skin, muscle, and fat, were used for these experiments.[28] Prior to use, the thickness of each filter was measured using a digital caliper at multiple locations to determine the average tissue thickness. Then, the sample was loaded into the photolysis flow cell and placed directly in front of the PD. Control experiments confirmed that photolysis of porcine skin, muscle, or fat alone did not result in NO release.

An important question is how well do these tissue samples transmit the 980 nm excitation light. Transmittance was measured by using a power meter to determine attenuation of the expanded NIR laser beam. In this manner, it was shown that the transmittance of a muscle sample (~2.7 mm thick) was 30% (abs = ~0.5), while that of fat (~2 mm) and skin (~2.6 mm) samples were 16 and 13%, respectively. Similar power losses were seen using a stationary, focused beam, although as noted above, muscle tissue in particular was damaged after short exposure under those conditions.

Figure 9 depicts the production of NO upon 980 nm photolysis of UCNP_RBS_PDs C(Tm), using the oscillating focused beam at 400 W cm^{-2} through a filter composed of porcine muscle tissue ~1.5 mm thick. Although the signals are significantly attenuated relative to the "unfiltered" experiment, NO is generated in very significant quantities. Similar photolysis of the A(Er) PD through thicker tissue filters, porcine skin (~2.6 mm), muscle (~2.7 mm), and fat (~2 mm) filters with the stationary beam at 28 W cm^{-2} and with the oscillating beam at 400 W cm^{-2} led in each case to quantifiable NO release (Table 3, Figures S-18 to S-20 of the Supporting Information). Not surprisingly, the quantities of NO generated were further attenuated. Interestingly, both the muscle and fat tissue samples seemed to increase in 980 nm transparency during the experiment, even though there was no visible damage to the tissue. We speculate that the arid conditions in the photolysis cell due to the He flow gas affected the tissue morphology, leading to changes in transparency. Another observation was the significantly slower return to baseline of the NOA signal after photolysis of PD A(Er) through the fat filter, suggesting that fat may absorb some NO and subsequently slowly releases it.

Table 3. Quantitative NO Data Generated from 980 nm Photolysis of A(Er) through Three Different Porcine Tissue Samples As Filters[a]

tissue filter	photolysis time (s)	NO produced (pmol)
skin (~2.6 mm)	20	7
	40	13
	80	25
	160	48
muscle (~2.7 mm)	20	9
	40	19
	80	59[b]
fat (~2 mm)	20	27[b]
	20(x4)	114[b]

[a]In each case, the focal point power density of the oscillating laser beam was 400 W/cm^2. The reported pmol NO detected is an average of three identical irradiation intervals. [b]Indicates that successive irradiation intervals of the same time consistently resulted in increasing amounts of NO detected.

Direct comparison of NO release from A(Er) in the presence and absence of tissue was not possible due to high power densities saturating the NOA in the absence of such filters, while in the presence of tissue the lower power densities did not generate an NO response. Additionally, factors such as variation in thickness, beam pattern and alignment, and the possible morphology changes of the muscle and fat during experiments prevented direct quantitative comparison of the relative transparency of each tissue sample. The important point is that both the A(Er) PD and C(Tm) PD were capable of generating physiologically relevant levels of NO,[29] upon irradiation through skin, muscle, and fat tissue.

dx.doi.org/10.1021/ja408516w | J. Am. Chem. Soc. 2013, 135, 18145−18152

SUMMARY

Photolysis of all the UCNP_RBS_PDs device formulations reproducibly released quantities of NO ranging from a few picomoles up to a few nanomoles, where the limiting factor on the high end was saturation of the NOA detector. Thus, given the marked sensitivity of the mammalian cardiovascular system to NO,[29] it is clear that each UCNP_RBS_PDs is capable of releasing biologically relevant amounts of NO from these solid-state devices under NIR irradiation with a simple CW diode NIR laser.[30] This is also the case for the through tissue experiments, although the NO production was significantly attenuated, in part due to the absorptivity of the tissue samples used but very likely also due to scattering mechanisms that tended to defocus the NIR beam. The use of the novel oscillating focused laser beam optical train provides a proof-of-principle demonstration of how to generate high local power densities for the purpose of accentuating this nonlinear process without damaging the tissue or the PD.[31] The nonlinear behavior with regard to both the oscillation frequency and the irradiation time intervals, although complicated, offers intriguing engineering possibilities for optimizing these systems for phototherapeutics. Future studies will be directed toward such optimization.

ASSOCIATED CONTENT

Supporting Information

Detailed synthesis and characterization of the UCNPs, assembly of the PDs, as well as development of the photolysis apparatus used. This material is available free of charge via the Internet at http://pubs.acs.org.

AUTHOR INFORMATION

Corresponding Author

E-mail: ford@chem.ucsb.edu

Author Contributions

[⊥]P.T.B. and J.V.G. contributed equally to this work

Notes

The authors declare no competing financial interest.

ACKNOWLEDGMENTS

This work was supported by the National Science Foundation (Grant NSF-CHE-1058794). We thank the Molecular Foundry User Program and especially Drs. Emory Chan and Alexis Ostrowski of the Molecular Foundry for assistance with the WANDA synthesis of UCNPs. Syntheses at the Molecular Foundry were supported by the Office of Science, Office of Basic Energy Sciences, of the U.S. Department of Energy under Contract no. DE-AC02-05CH11231. P.T.B. thanks the ConvEne-IGERT program at UCSB (NSF-DGE 0801627) and J.V.G. thanks the PIRE-ECCI (Grant NSF-OISE-0968399) program at UCSB for graduate fellowships. R.G. and J.T. thank the IRES-ECCI program at UCSB (Grant NSF-OISE-1065581) for undergraduate fellowships. P.T.B. and J.T. thank Suzhou Institute of Nanotech and Nanobionics (SINANO), Chinese Academy of Sciences, China for aid in the TEM studies. P.T.B. and J.V.G. thank Richard Bock and Bruce Dunson of UCSB for assistance fabricating the photolysis apparatus.

REFERENCES

(1) (a) Furuta, T.; Wang, S. S.-H.; Dantzker, J. L.; Dore, T. M.; Bybee, W. J.; Callaway, E. M.; Denk, W.; Tsien, R. Y. *Proc. Natl. Acad. Sci. U.S.A.* **1999**, *96*, 1193−1200. (b) Ford, P. C. *Acc. Chem. Res.* **2008**, *41*, 190−200. (c) Ciesienski, K. L.; Franz, K. J. *Angew. Chem., Int. Ed.* **2011**, *50*, 814−824.

(2) (a) Smith, A. M.; Mancini, M. C. *Nat. Nanotechnol.* **2009**, *4*, 710−711. (b) Matsuzaki, M.; Hayama, T.; Kasai, H.; Ellis-Davies, G. C. R. *Nat. Chem. Biol.* **2010**, *6*, 255−257. (c) Yang, Y.; Shao, Q.; Deng, R.; Deng, R.; Wang, C.; Teng, X.; Cheng, K.; Cheng, Z.; Huang, L.; Liu, Z.; Liu, X.; Xing, B. *Angew. Chem., Int. Ed.* **2012**, *51*, 3125−3129. (d) Yan, B.; Boyer, J.-C.; Habault, D.; Branda, N. R.; Zhao, Y. *J. Am. Chem. Soc.* **2012**, *134*, 16558−16561. (e) Chien, Y.-H.; Chou, Y.-L.; Wang, S.-W.; Hung, S.-T.; Liau, M.-C.; Chao, Y.-J.; Su, C.-H.; Yeh, C.-S. *ACS Nano* **2013**, *7*, 8516−8528.

(3) Garcia, J. V.; Zhang, F.; Ford, P. C. *Philos. Trans. R. Soc., A* **2013**, *371* (1995), 20120129.

(4) (a) Auzel, F. *Chem. Rev.* **2003**, *104*, 139−174. (b) Auzel, F. E. *Proc. IEEE* **1973**, *61*, 758−786. (c) Haase, M.; Schäfer, H. *Angew. Chem., Int. Ed.* **2011**, *50*, 5808−5829. (d) Wang, C.; Cheng, L.; Liu, Z. *Theranostics* **2013**, *3*, 317−330.

(5) (a) Kudo, S.; Bourassa, J. L.; Boggs, S. E.; Sato, Y.; Ford, P. C. *Anal. Biochem.* **1997**, *247*, 193−202. (b) Bourassa, J.; Lee, B.; Bernhard, S.; Schoonover, J.; Ford, P. C. *Inorg. Chem.* **1999**, *38*, 2947−2952. (c) Chmura, A.; Szacilowski, K.; Waksmundzka-Gora, A.; Stasicka, Z. *Nitric Oxide* **2006**, *14*, 247−260.

(6) (a) Szabo, C. *Sci. Transl. Med.* **2010**, *2*, 59ps54. (b) Fukuto, J. M.; Carrington, S.; Tantillo, D. J.; Harrison, J.; Ignarro, L.; Freeman, B. A.; Chen, A.; Wink, D. A. *Chem. Res. Toxicol.* **2012**, *25*, 769.

(7) (a) *Nitric Oxide: Biology and Pathobiology*, 2nd ed.; Ignarro, L. J., Ed.; Elsevier Inc.: Burlington, MA, 2010. (b) Wink, D. A.; Mitchell, J. B. *Free Radical Biol. Med.* **1998**, *25*, 434−456.

(8) (a) Mitchell, J. B.; Wink, D. A.; DeGraff, W.; Gamson, J.; Keefer, L. K.; Krishna, M. C. *Cancer Res.* **1993**, *53*, 5845−5848. (b) Bourassa, J.; DeGraff, W.; Kudo, S.; Wink, D. A.; Mitchell, J. B.; Ford, P. C. *J. Am. Chem. Soc.* **1997**, *119*, 2853−2860. (c) Jordan, B. F.; Sonveaux, P.; Feron, O.; Gregoire, V.; Beghein, N.; Dessy, C.; Gallez, B. *Int. J. Cancer* **2004**, *109*, 768−773. (d) Nagane, M.; Yasui, H.; Yamamori, T.; Zhao, S.; Kuge, Y.; Tamaki, N.; Kameya, H.; Fujii, H.; Inanami, O. *Biochem. Biophys. Res. Commun.* **2013**, *437*, 420−425.

(9) Examples are (a) Saavedra, J. E.; Billiar, T. R.; Williams, D. L.; Kim, Y. M.; Watkins, S.; Keefer, L. K. *J. Med. Chem.* **1997**, *40*, 1947−195. (b) Ostrowski, A. D.; Ford, P. C. *Dalton Trans.* **2009**, 10660−10669. (c) Burks, P. T.; Ostrowski, A. D.; Mikhailovsky, A. A.; Chan, E. M.; Wagenknecht, P. S.; Ford, P. C. *J. Am. Chem. Soc.* **2012**, *134*, 13266−13275. (d) Burks, P. T.; Ford, P. C. *Dalton Trans.* **2012**, *41*, 13030−13042. (d) Rose, M. J.; Mascharak, P. K. *Curr. Opin. Chem. Biol.* **2008**, *12*, 238−244. (e) Sortino, S. *J. Mater. Chem.* **2012**, *22*, 301−318.

(10) (a) Nichols, S. P.; Storm, W. L.; Koh, A.; Schoenfisch, M. H. *Adv. Drug Delivery Rev.* **2012**, *64*, 1177−1188. (b) Tfouni, E.; Doro, F. G.; Gomes, A. J.; Silva, R. S. d.; Metzker, G.; Benini, P. G. a. Z.; Franco, D. W. *Coord. Chem. Rev.* **2010**, *254*, 355−371. (c) Frost, M. C.; Reynolds, M. M.; Meyerhoff, M. E. *Biomater* **2005**, *26*, 1685−1693. (d) Marxer, S. M.; Rothrock, A. R.; Nablo, B. J.; Robbins, M. E.; Schoenfisch, M. H. *Chem. Mater.* **2003**, *15*, 4193−4199. (e) Li, Y. Y.; Cunin, F. d. r.; Link, J. R.; Gao, T.; Betts, R. E.; Reiver, S. H.; Chin, V.; Bhatia, S. N.; Sailor, M. J. *Science* **2003**, *299*, 2045−2047.

(11) (a) Smith, A. M.; Mancini, M. C.; Nie, S. *Nat. Nanotechnol.* **2009**, *4*, 710. (b) König, K. *J Microsc.* **2000**, *200*, 83.

(12) (a) Wecksler, S. R.; Mikhailovsky, A.; Korystov, D.; Ford, P. C. *J. Am. Chem. Soc.* **2006**, *128*, 3831−3837. (b) Wecksler, S. R.; Mikhailovsky, A.; Korystov, D.; Buller, F.; Kannan, R.; Tan, L.-S.; Ford, P. C. *Inorg. Chem.* **2007**, *46*, 395−402.

(13) Garcia, J. V.; Yang, J.; Shen, D.; Yao, C.; Li, X.; Wang, R.; Stucky, G. D.; Zhao, D.; Ford, P. C.; Zhang, F. *Small* **2012**, *8*, 3701−3701.

(14) (a) Zheng, Q.; Bonoiu, A.; Ohulchanskyy, T. Y.; He, G. S.; Prasad, P. N. *Mol. Pharmaceutics* **2008**, *5*, 389−98. (b) Hishikawa, K.; Nakagawa, H.; Furuta, T. *J. Am. Chem. Soc.* **2009**, *131*, 7488.

(15) (a) Chatteriee, D. K.; Rufalhah, A. J.; Zhang, Y. *Biomaterials* **2008**, *29*, 937−943. (b) Dong, N.-N.; Pedroni, M.; Piccinelli, F.;

Conti, G.; Sbarbati, A.; Ramirez-Hernandez, J. E.; Maestro, L. M.; Iglesias-de la Cruz, M. C.; Sanz-Rodriguez, F.; Juarranz, A.; Chen, F.; Vetrone, F.; Capobianco, J. A.; García Solé, J.; Bettinelli, M.; Jaque, D.; Speghini, A. *ACS Nano* **2011**, *5*, 8665−8671. (c) Wang, F.; Raval, Y.; Chen, H.; Tzeng, T.-R. J.; DesJardins, J. D.; Anker, J. N. *Adv. Healthcare Mater.* **2013**, DOI: 10.1002/adhm.201300101.

(16) (a) Abbasi, F.; Mirzadeh, H.; Katbab, A.-A. *Polym. Int.* **2001**, *50*, 1279−1287. (b) Belanger, M.-C.; Marois, Y. *J. Biomed. Mater. Res.* **2001**, *58*, 467−477.

(17) Food and Drug Administration, 21CFR173.340. CFR-Code of Federal Regulations Title 21. http://www.accessdata.fda.gov/scripts/cdrh/cfdocs/cfcfr/CFRSearch.cfm?fr=173.340 (revised 04/01/13, accessed 06/03/13).

(18) (a) McDonald, J. C.; Whitesides, G. M. *Acc. Chem. Res.* **2002**, *35*, 491−499. (b) Polmanteer, K. E. *Rubber Chem. Technol.* **1988**, *61*, 470−502. (c) Baltussen, E.; Cramers, C. A.; Sandra, P. J. F. *Anal. Bioanal. Chem.* **2002**, *373*, 3−22. (d) Simmons, A.; Padsalgikar, A. D.; Ferris, L. M.; Poole-Warren, L. A. *Biomaterials* **2008**, *29*, 2987−2995.

(19) Su, Q.; Han, S.; Xie, X.; Zhu, H.; Chen, H.; Chen, C.-K.; Liu, R.-S.; Chen, X.; Wang, F.; Liu, X. *J. Am. Chem. Soc.* **2012**, *134*, 20849−20857.

(20) Chan, E. M.; Xu, C.; Mao, A. W.; Han, G.; Owen, J. S.; Cohen, B. E.; Milliron, D. *J. Nano Lett.* **2010**, *10*, 1874−1885.

(21) Ostrowski, A. D.; Chan, E. M.; Gargas, D. J.; Katz, E. M.; Han, G.; Schuck, P. J.; Milliron, D. J.; Cohen, B. E. *ACS Nano* **2012**, *6*, 2686−2692.

(22) Wang, F.; Han, Y.; Lim, C. S.; Wang, J.; Xu, J.; Chen, H.; Zhang, C.; Hong, M.; Liu, X. *Nature* **2010**, *463*, 1061−1064.

(23) Chan, E. M.; Han, G.; Goldberg, J. D.; Gargas, D. J.; Ostrowski, A. D.; Schuck, P. J.; Cohen, B. E.; Milliron, D. J. *Nano Lett.* **2012**, *12*, 3839−3845.

(24) Boyer, J.-C.; van Veggel, F. C. J. M. *Nanoscale* **2010**, *2*, 1417−1419.

(25) PDs were loaded with 0, 1, 2, 3, 5 or 10 mg of UCNPs; testing for NO release under 980 nm excitation established 5 mg UCNP (∼11% by weight of the ∼45 mg total mass) to give the most efficient behavior of these devices. Those with higher loading gave lower NO release, a likely result of increased UCNP aggregation.

(26) Beam intensities are calculated from the adjustable output power of the laser (in Watts) divided by the area at the focal point (5×10^{-3} cm^2). Beam diameter was measured using the Foucault knife-edge method with an apparatus engineered in our laboratory.

(27) Heating effects can be discounted since spreading a stationary beam to encompass the same surface area of the UCNP_RBS_PD that the oscillating beam addresses and using the same total power does produce some NO (Figure 3) but only a fraction of that generated in the latter case for longer excitation intervals.

(28) Tissue samples were acquired from a local butcher. Skin was from a pork shoulder, muscle came from pork tenderloin, and fat came from bacon.

(29) (a) Garthwaite, J. *Mol. Cell. Biochem.* **2010**, *334*, 221−232. (b) Bellamy, T. C.; Griffiths, C.; Garthwaite, J. *J. Biol. Chem.* **2002**, *277*, 31801−31807.

(30) (a) During the preparation of this article, we learned of an independent study in another laboratory (ref 29b) that used PDMS films incorporating UCNPs for the generation of NO from nitric oxide photochemical precursors. (b) Ostrowski A. D., personal communication, 2013.

(31) (a) In two recent reports (refs 30a and 30b), UCNPs have been formulated with added Nd^{3+} to make them more responsive to 800 nm excitation. Since this wavelength is absorbed less by water than by the 980 nm of light typically used with UCNPs, this may be another approach to reducing potential tissue damage from the NIR excitation lasers. (b) Shen, J.; Chen, G.; Vu, A.-M.; Fan, W.; Bilsel, O. S.; Chang, C.-C.; Han, G. *Advanced Optical Materials* **2013**, *1*, 644−650. (c) Xie, X.; Gao, N.; Deng, R.; Sun, Q.; Xu, Q.-H.; Liu, X.-G. *J. Am. Chem. Soc.* **2013**, *135*, 12608−12611.